



Reusable Mg–Al hydrotalcites for the catalytic synthesis of diglycerol dicarbonate from diglycerol and dimethyl carbonate



Joseph A. Stewart, Bert M. Weckhuysen, Pieter C.A. Bruijninx*

Inorganic Chemistry and Catalysis, Debye Institute for Nanomaterials Science, Utrecht University, Universiteitsweg 99, 3584 CG Utrecht, The Netherlands

ARTICLE INFO

Article history:

Received 10 March 2014

Received in revised form 24 May 2014

Accepted 23 June 2014

Available online 31 July 2014

Keywords:

Diglycerol

Diglycerol dicarbonate

Hydrotalcites

Non-isocyanate polyurethanes

ABSTRACT

Diglycerol dicarbonate, which has been highlighted as a potential monomer for the production of non-isocyanate polyurethanes, has been synthesised using as-synthesised hydrotalcites of varying magnesium-to-aluminium ratio as catalyst materials. The hydrotalcite materials were aged for two different times, influencing their crystallite size. The catalytic carbonylation of diglycerol into diglycerol dicarbonate with dimethyl carbonate as “CO” source and solvent, ran to full conversion within 6 h, with complete selectivity, operating at relatively mild temperatures. Diglycerol monocarbonate was observed as a reaction intermediate in this conversion process. The increased basicity observed with increasing Mg/Al ratio led to higher activities. The catalysts can be easily recovered and re-used without any further activation treatment, whilst still displaying their high activity.

© 2014 Elsevier B.V. All rights reserved.

1. Introduction

Glycerol is considered an important renewable platform molecule for the synthesis of various bulk and specialty chemicals [1,2]. It is traditionally produced in large amounts by simple hydrolysis of triglycerides [3]. More recently, large volumes of glycerol are also being produced as a by-product of biodiesel production by trans-esterification, with about 110 kg of crude glycerol being produced per ton of biodiesel. This has led to a surplus of glycerol flooding the market, with traditional outlets such as pharmaceuticals, the food industry and solvents, not being able to make use of this excess. Even though the longer-term viability of biodiesel production from oils and fats is debateable, current production projections still forecast a growth in Europe of about 140 million metric tons between 2030 and 2050 [4]. Moreover, glycerol is expected to play a major role in future biorefinery systems. The effect of this new and growing glycerol source is that the readily available glycerol becomes inexpensive, with some projections suggesting the price could be as low as \$0.11 per kg for crude glycerol solutions [5]. This in turn makes the development of new glycerol-based products very attractive and a number of technologies have indeed been developed recently for conversion of glycerol to value-added chemicals.

Examples include the conversion of glycerol into glyceric acid by oxidation [6–9], propylene glycol and 1,3-propanediol by hydrogenolysis [10–14] and acrolein by dehydration [15–19]. In recent years, extensive research has also been carried out investigating the production of glycerol carbonate (GC) from glycerol [20]. GC can be used in a number of ways; applications range from renewable solvents and beauty products to building eco-composites to charge carriers in lithium batteries. It has already been incorporated into a number of companies' portfolios due to its attractive physical properties and reactivity. The advantages of using GC include it being non-flammable, non-toxic and biodegradable as well as water-soluble. GC derivatives have also been highlighted for potential use as monomers for non-isocyanate polyurethanes (NIPUs) [21].

Glycerol itself can also be condensed to dimers and oligomers [22], for instance, by catalytic etherification with simple alkaline or alkaline earth-based bases [23]. These highly functional molecules can in turn be used as or converted into multifunctional building blocks, such as cyclic carbonates, for the production of various polymers. The possibility of producing polyurethanes, a class of polymer in high demand, via a phosgene-free route by utilising these cyclic carbonates derived from glycerol holds great potential, for example [24]. In fact, diglycerol dicarbonate has been highlighted as a very desirable building block for this process [21].

While various routes have been reported and are being used for the production of glycerol carbonate [25–27], no catalytic routes to diglycerol dicarbonate have been reported to date. Phosgene has previously been used for the production of GC from glycerol, but its

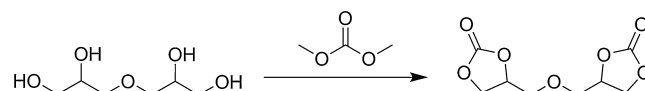
* Corresponding author. Tel.: +31 302537400; fax: +31 302511027.
E-mail address: p.c.a.bruijninx@uu.nl (P.C.A. Bruijninx).

highly toxic nature has led to research into more environmentally friendly processes [28]. It has been shown that a number of different catalytic systems can be utilised for this process, as well as a range of “CO” sources. Direct synthesis from glycerol and CO₂ would appear to be a favourable route, as this would make the resulting glycerol carbonate 100% renewable; to date, glycerol conversions of only 35% have been achieved, however, which is attributed to the unfavourable thermodynamics of the reaction [29,30]. Alternatives to CO₂ have also widely been investigated. One such source is simply carbon monoxide for which good yields have been recorded in oxidative carbonylation reactions for a number of systems [31,32]. Transcarbonation, the carbonyl exchange reaction between alcohols and CO sources, of which phosgene is one example, holds a greater potential. Other than phosgene, two other classes of CO sources have been used in the synthesis of GC, namely dialkyl carbonates and cyclic carbonates such as ethylene and propylene carbonate, both of which have shown good conversion with a range of basic catalysts at relatively mild temperatures of around 100 °C [25,33,34].

Both homogeneous and heterogeneous catalyst systems have been reported for the formation of cyclic carbonates with various CO sources. These range from ionic liquids [35] to transition metal complexes [32] and supported metal catalysts [36] to simple (mixed)-metal oxides [37,38]. The mixed oxides have been shown to be particularly versatile and could be used with each of the reagents mentioned above. A number of alkaline earth metal oxides and mixed oxides of, e.g., Zr, Mg, Al and Ca, demonstrate high activity for the formation of GC. Of particular interest is the use of Mg–Al hydrotalcites, basic materials that are often used as precursor in the synthesis of heterogeneous mixed oxide bases. Hydrotalcites (HTs) are naturally occurring layered anionic clays with the general formula $[M^{2+}_{1-x}M^{3+}_x(OH)_2]^{x+}A^{n-}_{x/n} \cdot mH_2O$, where M^{2+} and M^{3+} are di- and trivalent metal ions, and A^{n-} is the interlayer anion. The structure consists of positively charged brucite-like layers with the anions, e.g. hydroxide or carbonate anions, being intercalated between these layers compensating the positive charge caused by the introduction of the trivalent ions [39]. Upon heat treatment (i.e., when exposed to temperatures higher than 400 °C), these hydrotalcites lose their ordered structure and become mixed oxides. For hydrotalcites, basicity can be manipulated by varying the Mg–Al ratio. Increasing the number of M^{3+} species decreases the density of basic sites [40].

Climent et al. have demonstrated the use of various mixed oxides, including Mg–Al mixed oxides of varying Mg–Al ratio obtained by calcination of their hydrotalcite precursors, for the transesterification of ethylene carbonate with glycerol to form GC. They were able to achieve 85% conversion within 5 h with 96% selectivity at 50 °C with a Mg–Al mixed oxide of ratio 3:1 [25]. It was furthermore shown that the initial rates of the mixed oxide and a rehydrated HT were very similar, indicating that Brønsted basic sites are as active for the reaction. Interestingly, Takagaki and co-workers showed that as-synthesised, uncalcined hydrotalcites with Mg–Al ratios from 2 to 5 are indeed also active catalysts for the synthesis of GC from glycerol and DMC using DMF as a solvent. High turnover numbers were observed for the catalysts with a Mg–Al ratio of 3 to 5:1, with the catalyst with a nominal ratio of 5:1 (measured as 4.31) generating the highest GC yield of 75% at 100 °C. The authors indicated that the presence of hydromagnesite in the higher Mg–Al ratio catalysts, while being inactive itself, has a positive influence of the activity [26].

As evidenced by the examples listed above, to date only the catalytic conversion of glycerol to glycerol carbonate has been reported. However, for use in polymers, multifunctional monomers are needed making the conversion to diglycerol dicarbonate (DGDC) from diglycerol (DG) also of interest (Scheme 1). In this paper, we demonstrate that full conversion to DGDC can



Scheme 1. Reaction scheme of diglycerol to diglycerol dicarbonate utilising DMC as the CO source.

be achieved within 6 h using as-synthesised hydrotalcites and dimethyl carbonate as CO source as well as solvent. We will also show that these heterogeneous catalysts can easily be recovered and reused, whilst still maintaining their original selectivity.

2. Experimental

2.1. Materials

Commercial hydrotalcites were purchased from Sasol, dimethyl carbonate from Merck ($\geq 99\%$), anisole (99%), magnesium nitrate hexahydrate (99+%) and aluminium nitrate nonahydrate (99+%) from Acros and sodium carbonate decahydrate (99%) and sodium hydroxide (99%) were purchased from Sigma Aldrich. All materials were used as-received without further purification. Diglycerol ($>80\%$) purchased from ABCR and shown by GC analysis to contain around 86% diglycerol and 5% glycerol, with the rest made up of higher oligomers.

2.2. Catalyst synthesis

Mg–Al hydrotalcites were prepared using an adapted literature coprecipitation method [26]. Mg–Al hydrotalcites of a nominal Mg/Al ratio of 2 and 5 were prepared by adding a solution of $Mg(NO_3)_2 \cdot 6H_2O$ (50 or 20 mmol) and $Al(NO_3)_3 \cdot 9H_2O$ (10 mmol) mixed in 100 mL deionised water dropwise to an alkaline solution of $Na_2CO_3 \cdot 10H_2O$ (30 mmol) and NaOH (70 mmol) in 60 mL deionised water. This mixture was then stirred at 60 °C for 1 h, before increasing the temperature to 100 °C and stirring for a further 2 or 22 h as indicated. After the pre-determined time, the white precipitate was filtered and washed with copious amounts of distilled water. Samples were dried overnight at 120 °C before being sieved to a 212–425 μm sieve fraction.

Hydromagnesite ($Mg_5(CO_3)_4(OH)_2 \cdot 4H_2O$) was prepared by adding slowly a 1 M aqueous solution of $Mg(NO_3)_2 \cdot 6H_2O$ (10 mmol) to a 1 M aqueous solution of $Na_2CO_3 \cdot 10H_2O$ (6 mmol) and allowing it to stir at 45 °C for 24 h. The white precipitate was filtered, washed with distilled water and dried at 120 °C overnight [41].

2.3. Catalytic testing

Typical catalytic reactions were carried out in closed 8 mL glass vials. To diglycerol (2 mmol) was added dimethyl carbonate (20 mmol) and 0.1 g catalyst. The reaction was stirred at 130 °C for the desired reaction time, after which the reaction was cooled in a water bath and filtered using a 30 μm filter. The filtered catalyst was washed with acetone and the washing collected and added to the reaction mixture. The acetone was then removed *in vacuo* at 40 °C. 0.5 mL of anisole was added as internal standard for NMR measurements, which were made in DMSO- d_6 .

2.4. Characterisation and analysis

Thermal instability of the product, DGDC, prevented the use of gas chromatography as an analytical tool. Reactions were thus evaluated by NMR with the use of anisole as internal standard and compared to an authentic sample of DGDC.

NMR analysis: 1H and ^{13}C NMR spectroscopic measurements were conducted at 25 °C on a Varian Oxford AS400 MHz

Table 1
Physicochemical properties of the self-synthesised and commercial hydrotalcites under study.

Catalyst	Nominal Mg/Al atom ratio	Actual Mg/Al ^a atom ratio	Surface area (m ² /g) ^b	Base sites ^c (μmol/g)
Mg1	Commercial	1.27	11.5	13.3
Mg2a	2	2.37	70.5	15.9
Mg2b	2	2.25	63.1	n.d.
Mg3	Commercial	2.95	14.1	18.1
Mg5a	5	4.74	80.2	32.0
Mg5b	5	5.21	58.9	n.d.

n.d., not determined.

^a Measured by ICP.

^b Measured by N₂-physisorption and calculated by BET method.

^c Measured using CO₂-TPD.

spectrometer. Chemical shifts (δ) are given in ppm referenced to the residual solvent signal.

Diglycerol: ¹H NMR (400 MHz, DMSO-d₆) δ = 4.60 (dd, 2H, CHOH), 4.46 (t, 2H, CH₂OH), 3.55 (m, 2H, CH), 3.39 (m, 4H, CHOH), 3.31 (m, 4H, CH₂O) ppm.

Diglycerol dicarbonate: ¹H NMR (400 MHz, DMSO-d₆) δ = 4.94 (m, 2H) CH(CH₂)₂O, 4.52 (t, 2H) and 4.23 (q, 2H) CH₂(O)CH, 3.73 (m, 4H) CH₂(O)CH ppm.

¹³C NMR (400 MHz, DMSO-d₆) δ = 65.90 (CH(O)CH₂O), 70.36 and 70.40 (C(O)CH(O)), 75.36 and 75.42 (CH(O)CH(O)C), 154.83 and 154.88 (C(O)OO) ppm.

TGA: Thermal gravimetric analysis was performed on a TA instrument Q50, by heating approximately 15 mg of sample to 120 °C at 5 °C/min and holding for 20 min then continuing to heat to 600 °C at 5 °C/min under a N₂ flow of 60 mL/min.

N₂: N₂-physisorption isotherms were recorded with a Micromeritics Tristar 3000 at 77 K. The samples were dried prior to performing the measurements for at least 16 h at 393 K in a N₂ flow. The surface area was determined using the Brunauer–Emmett–Teller (BET) theory. The total pore volume was defined as the single-point pore volume at $p/p_0 = 0.95$.

ICP: Inductively coupled plasma measurements were performed at Mikroanalytisches Labor Kolbe, Mülheim, Germany.

XRD: Powder X-ray diffraction (XRD) patterns were obtained by a Bruker-AXS D2 Phaser powder X-ray diffractometer using Co K $\alpha_{1,2}$, with $\lambda = 1.79026$. Measurements were carried out between 8° and 99° 2 θ using a step size of 0.05° 2 θ and a scan speed of 1.5 s.

CO₂ adsorption: Volumetric CO₂ adsorption measurements in the pressure range 0–1 mbar were performed at 0 °C using a Micromeritics ASAP2000. Samples were pre-dried at 120 °C under a vacuum of 1 μbar overnight.

3. Results and discussion

3.1. Catalyst synthesis and characterisation

A series of Mg–Al hydrotalcite catalysts were synthesised using an adapted co-precipitation method [26]. Hydrotalcites of targeted Mg/Al ratios of 2 and 5 were synthesised with two different ageing times of 2 and 22 h at 100 °C, which followed an initial 1 h of stirring at 60 °C. The ageing steps at elevated temperature are not included in the synthesis method of Takagaki et al. [26], in which the samples are only aged at a temperature of 65 °C, but has previously been implemented in another literature procedure [42]. The purpose of the two different ageing times was to assess the influence on catalytic performance of crystallite size and of hydromagnesite in the structure of the hydrotalcites with a Mg/Al ratio of 5. Indeed, Takagaki et al. [26] previously observed a beneficial effect of some hydromagnesite (Mg₅(CO₃)₄(OH)₂·4H₂O) that was incorporated in their HT materials, even though the hydromagnesite itself was inactive in glycerol carbonate formation. The synthesised hydrotalcites are described throughout the paper with their target Mg/Al ratio

and either ‘a’ for 2 h ageing or ‘b’ for 22 h ageing, e.g. **Mg2a** represents a target ratio of Mg/Al 2 and underwent a 2 h ageing treatment at 100 °C. The actual Mg/Al ratios as determined by ICP are given in Table 1 and found to be close to the target values, indicating that the synthesis was successful. The results obtained in DGDC synthesis with the self-synthesised HTs were benchmarked against commercial samples, whose Mg/Al ratios fell in between the self-synthesised ones. These commercial hydrotalcites are denoted as **Mg1** and **Mg3**, with the number representing the nearest integer to the measured Mg/Al ratio. Each of the synthesised and commercial samples possessed the typical hydrotalcite structure, as observed with XRD (Fig. 1). As expected, the samples with a magnesium-to-aluminium target ratio of 5 also contained diffraction peaks of a hydromagnesite phase (Fig. 2), with this phase being more intense in the XRD pattern of the **Mg5b** sample; this corresponds to the findings of Takagaki et al. who found that Mg/Al ratios above 4 led to excess magnesium cations being precipitated as hydromagnesite under their synthesis conditions, and its formation being a function of ageing time [26]. Indeed, while Mg/Al ratios of 2–5 are typically reported for both HTs and HT-derived mixed oxides, more control over the actual Mg–Al ratio is achieved for those with a ratio lower than 4 [43]. As expected, crystallite size of the materials is also influenced by ageing time (see below), as can be easily seen by the sharpening of, e.g., the (003) and (006) reflections at around 13° and 27° 2 θ upon increased ageing time. A comparison of samples prepared with the same ageing time shows smaller crystallite sizes for **Mg5** samples, which can probably be ascribed to the presence of the hydromagnesite phase, an effect that has been observed before [26]. The average crystallite size, calculated using Scherrer’s equation on the (003) reflection, increased with longer ageing times for both

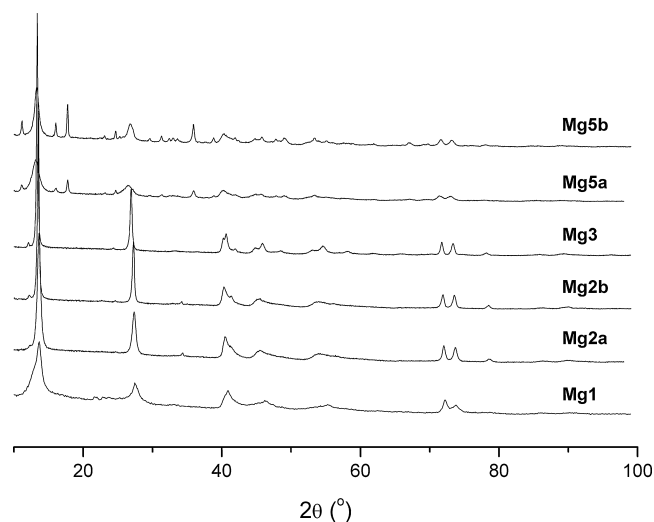


Fig. 1. XRD patterns of both self-synthesised and commercial hydrotalcites under study.

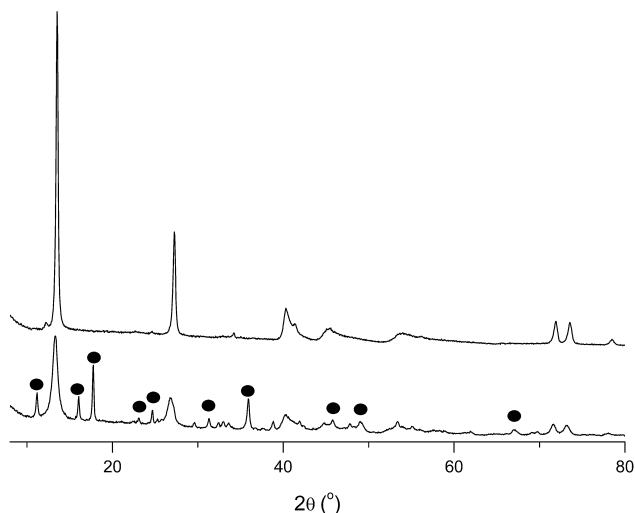


Fig. 2. XRD patterns of the fresh hydrotalcite materials **Mg2b** (top) and **Mg5b** (bottom)—circles represent hydromagnesite incorporated into the HT structure [26].

Mg2 and **Mg5** samples, from 15 to 32 nm and 8 to 12 nm, respectively. The less pronounced increase is in accordance with literature and has been ascribed to the influence of the hydromagnesite in the higher Mg–Al samples, with crystallite sizes of 12–24 and 9–10 nm being observed for samples of Mg–Al of 2 and 5, respectively [26]. The commercial sample **Mg3** had a larger crystallite size of 35 nm, similar to **Mg2b**.

TEM images (Fig. 3) of the synthesised hydrotalcites, however, show agglomerations of the crystallites, with ill-defined crystallite structures for the higher Mg–Al ratio materials being observed. The TEM images also show a higher proportion of needle-like particles for the higher Mg–Al ratio sample (**Mg5b**). The average particle size of 40 nm that is observed for **Mg5b** by TEM is smaller than the 74 nm that is seen for **Mg2b**. The average particle sizes from TEM are significantly bigger than the crystallite sizes extracted from the XRD patterns, given that XRD only probes the size of the crystalline domains of the agglomerated particles. The values are in good accordance with literature, however, with particle sizes of 100 nm having been reported for materials with a Mg/Al of 2 that were aged for 24 h at 100 °C based on SEM measurements [42]. The TEM images also confirm that the average particle size decreases with the longer ageing time for the materials with Mg/Al ratio of 5, presumably as a result of the extent of hydromagnesite formation. For the samples with lower Mg/Al ratio, the longer ageing time resulted in a higher average particle size of 74 nm compared with 45 nm, which is in accordance with literature that shows that with

increasing ageing time and temperature, particle size increases for hydrotalcites made with a co-precipitation method [42]. By contrast, the commercial catalyst has significantly larger average agglomerates and is poorly crystallised.

The BET surface areas of the self-synthesised catalysts indeed differed significantly from the commercial ones, with the latter showing considerably lower surface areas. As can be seen in Table 1, the surface areas of the commercial catalysts are 11.5 (**Mg1**) and 14.1 (**Mg3**) m²/g, while the surface areas for the self-synthesised ones range from 58.9 to 80.2 m²/g. The low surface areas of the commercial samples are attributed to the harsher, less-defined treatments that are undergone on the larger industrial scale.

Basicity of the hydrotalcites was assessed using CO₂-TPD to probe the number of Brønsted basic sites in the catalysts. As shown in Table 1, there is a general trend that as Mg/Al ratio increases the number of basic sites increases, which is in accordance with the literature [26]. As expected, the total number of basic sites is an order of magnitude lower than those reported for HTs that are obtained by calcination and reconstruction, but these are sufficient to efficiently catalyse the desired reaction, obviating the need for these additional catalyst preparation steps (see below) [44,45].

3.2. Catalyst testing

All hydrotalcites were tested for their activity in the carbonylation of diglycerol with dimethyl carbonate (DMC). Reactions were run at a temperature of 130 °C and under solventless conditions using a 10-fold excess of DMC as CO source (see Table 2 and Scheme 1). The excess DMC was used to help circumvent mixing issues arising from the viscosity of the diglycerol and the resulting product; a lower ratio of 5 to 1 was also found to result in good yields, though. Reactions were analysed using NMR spectroscopy, as the limited thermal stability of diglycerol dicarbonate (200 °C) does not allow product analysis by classical gas chromatographic analytical methods. Taking into account the boiling point of DMC (90 °C) and the decomposition temperature of DGDC, the excess DMC can easily be recovered through simple distillation. Full conversion was typically obtained after 6 h of reaction, which corresponds to a maximum DGDC yield of around 86%. Indeed, conversions as given in Table 2 are defined as amount of DG still observed in the NMR, whereas DGDC yields are defined assuming all starting material was DG (note that the starting diglycerol being impure, with the major impurities having been identified as glycerol (5%), triglycerol and other oligomers). Higher yields were obtained with increasing Mg/Al ratio, with all catalysts except **Mg1** yielding significant amounts of DGDC. The general trend is that yield increases with number of basic sites, an observation that is in line with the results reported by Takagaki et al. who reported

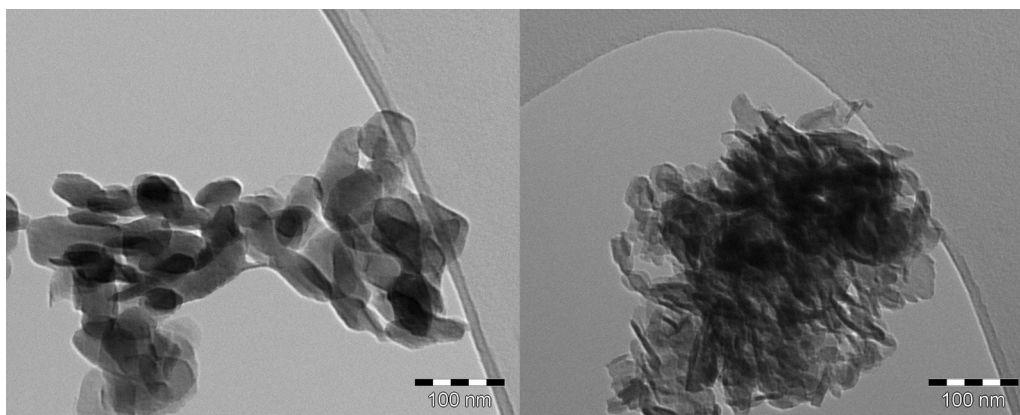


Fig. 3. TEM images of the synthesised hydrotalcites **Mg2b** (left) and **Mg5b** (right).

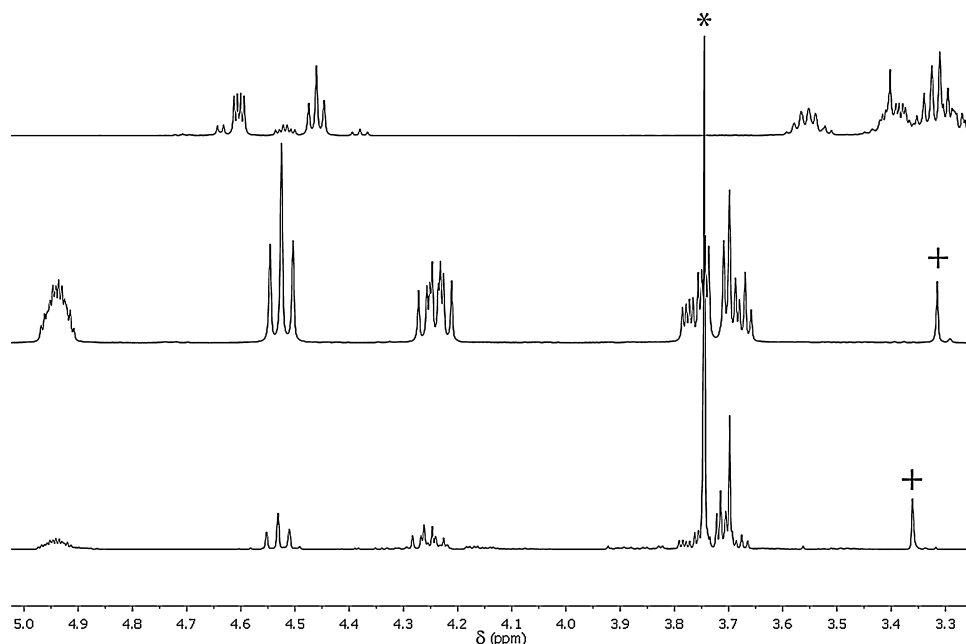


Fig. 4. ^1H NMR spectra in DMSO-d_6 of (top to bottom) the commercial diglycerol substrate, an authentic sample of diglycerol dicarbonate, and the reaction mixture of the catalyst material **Mg5a** showing the clean formation of diglycerol dicarbonate. * Peak from anisole internal standard; + Water peak.

Table 2
Catalytic performance of the hydrotalcites under study for the synthesis of diglycerol dicarbonate from diglycerol and dimethyl carbonate at a reaction temperature of 130°C .

Catalyst	Mg/Al atom ratio	Conversion (%)	DGMC Intermediate (%)	DGDC yield (%)	TONs
Mg1	1.27	37	18	3	361
Mg2a	2.37	86	14	68	1887
Mg2b	2.25	95	10	78	–
Mg3	2.95	95	15	73	1779
Mg5a	4.74	93	2	84	1063
Mg5b	5.21	97	0	86	–

Reaction conditions: 2 mmol of DG, 20 mmol of DMC, 0.1 g of catalyst, 6 h, 130°C .

the highest GC yield for a sample with Mg/Al ratio of 5 [26]. The reduced yield observed for **Mg3** can be attributed to the larger, less-defined crystallite size observed for the commercial catalyst. TONs of 361, 1887, 1779 and 1063 for **Mg1**, **Mg2a**, **Mg3** and **Mg5a**, respectively, are higher than those reported by Takagaki, with the highest TON (for a catalyst not at full conversion) achieved by **Mg2a**. The observed conversion for each catalyst is higher than the DGDC yield due to the fact that the reaction proceeds via the diglycerol monocarbonate intermediate DGMC (see Fig. 5). The more active catalysts, **Mg5a** and **Mg5b** reach the final product faster than the other catalysts, although conversion of diglycerol is similar. It is important to note that reactions run with a pure hydromagnesite material yielded as little as 4% DGDC under the same conditions. This phase is therefore not directly involved in catalysis, but its presence does seem to indirectly influence the number of accessible basic sites, as was again previously observed for GC production [26]. Reactions were also attempted with diethyl carbonate, for which Takagaki et al. and Alvarez et al. reported similar solid bases to catalyse glycerol carbonate formation [26,46]. Remarkably, only low yields were observed for **Mg2a** and **Mg2b** and little-to-no yield for the higher Mg/Al ratio hydrotalcites (data not shown).

The reaction itself is very selective, with no other diglycerol-derived products being observed as highlighted in Fig. 4, which shows the NMR spectrum of a reaction mixture of a run with **Mg5a** as well as the spectra of DG and an authentic sample of DGDC. While the NMR spectra obtained after 6 h of reaction only show the final product, the intermediate DGMC could be detected when the reaction was monitored over time by NMR (see Fig. 5, exemplified

by the reaction with **Mg3**). The assignment of the intermediate product is based on a multiplet that appeared at around 4.90 ppm, slightly upfield of the signal that is assigned to the tertiary protons of the product. We postulate that this shielded signal is from the

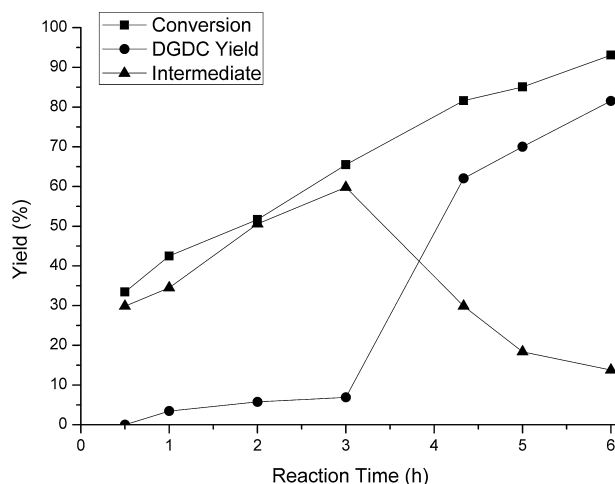


Fig. 5. Time profile of the **Mg3**-catalysed synthesis of diglycerol dicarbonate from diglycerol and dimethyl carbonate at a reaction temperature of 130°C under solvent-free conditions showing diglycerol conversion (squares), diglycerol dicarbonate yield (circles) and the reaction intermediate diglycerol monocarbonate DGMC (triangles).

Table 3
Catalyst reuse experiments for the catalyst materials **Mg3**, **Mg5a** and **Mg5b**.

Catalyst	Run	Conversion (%)	DGDC yield (%)	DGDC selectivity (%)
Mg3	1	95	73	77
	2	93	72	77
Mg5a	1	93	84	90
	2	91	74	81
	3	89	77	87
Mg5b	1	97	86	89
	2	86	74	86

Reaction conditions: 2 mmol of DG, 20 mmol of DMC, 0.1 g of catalyst, 6 h, 130 °C.

tertiary proton of the diglycerol mono-carbonate intermediate. As the reaction progressed, the signal at 4.90 ppm increased significantly before the signal at 4.94 ppm appeared and continued to grow. The signal at 4.90 ppm decreased again for longer reaction times. This can explain the initially observed difference between the observed conversion and DGDC yield (Fig. 5; conversion increased steadily over time, while DGDC yield remained low). The presence of this monocarbonate intermediate may explain the initially low DGDC yield and its rapid increase after 3 h. In catalytic GC synthesis, the open, mixed carbonate is also sometimes detected as intermediate [25]. We did not detect any open carbonate intermediates, however, indicating that the intramolecular ring-closing step is much faster than the first, mixed carbonate formation step with dimethyl carbonate under the applied conditions.

3.3. Catalyst re-use

A selected number of the catalyst materials under study, namely samples **Mg3**, **Mg5a** and **Mg5b**, were tested for re-use. Following each reaction, the catalyst material is filtered and washed with acetone. The spent catalyst was subsequently dried at 80 °C to remove any residual acetone. These recovered catalysts were then re-used in reactions run under the standard conditions. All three of the catalyst materials tested again achieved high yields, in the case of **Mg5a** even after multiple runs, as illustrated in Table 3. Activity decreases slightly of each of the catalyst materials, however **Mg5a** and **Mg5b** still maintain their original selectivity (note that a yield of 86% equates to fully selective conversion of DG to DGDC when taking into account the purity of the starting material). **Mg3** has lower selectivity towards the final product, even as a fresh catalyst, indicating that the transformation from the mono- to the dicarbonate is slower.

There are no significant differences detected in the XRD pattern of the fresh and spent catalyst, as can be seen for **Mg5a** in Fig. 6. There is slight broadening of the peaks observed at 13° and 27°,

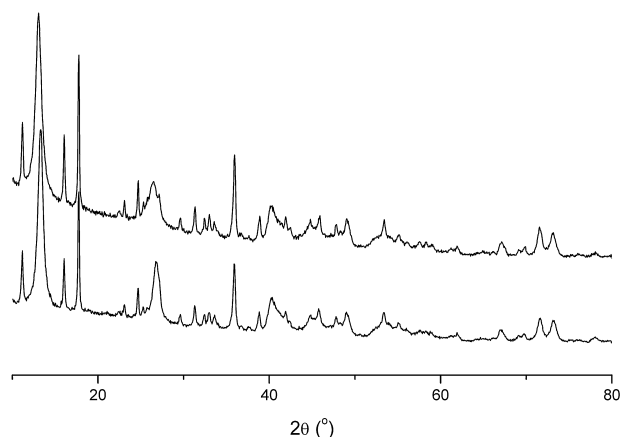


Fig. 6. XRD patterns of the fresh **Mg5a** (bottom) and spent **Mg5a** (top) catalyst materials.

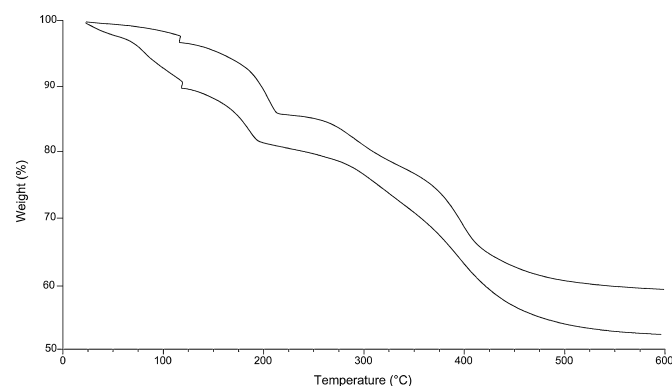


Fig. 7. Thermogravimetric analysis of the fresh **Mg3** (top) and spent **Mg3** (bottom) catalyst materials.

which equates to a decrease in crystallite size from 8 to 6 nm. No mixed oxide peaks were observed, as expected at these mild temperatures. There is also a decrease observed in particle size (e.g., from 50 to 33 nm for **Mg5a**) in the TEM images of the spent catalyst, with crystallites appearing more dispersed and fewer agglomerates being observed. TGA (Fig. 7) and IR (data not shown) measurements of the fresh and spent catalysts (data not shown) furthermore showed that there is very little “coke” deposited on the catalysts and after sufficient drying and removal of the acetone, the catalysts again exhibited high activity and retained their original selectivity. Indeed, no colouration of the catalyst was observed after its use. Fig. 7 shows that there is a minimal difference, 0.45%, between the fresh and spent catalyst for the weight loss above 120 °C. Weight loss below 120 °C is due to adsorbed water and acetone. The spent catalyst materials that were used in the re-use experiments were therefore dried at 80 °C to remove the acetone. The large weight loss observed above 180 °C in both the fresh and spent catalysts has been attributed to the loss of interlayer water (180–200 °C) and dehydroxylation and decarboxylation above 300 °C. Above 250 °C, the cationic layers also start to decompose [47].

4. Conclusions

An efficient synthesis of diglycerol dicarbonate from diglycerol and dimethyl carbonate is presented. This has been possible by using a series of hydrotalcite materials of varying magnesium-to-aluminium ratio as catalyst materials and full conversion could be achieved within 6 h at a reaction temperature of 130 °C. An increase in Mg/Al ratio leads to higher basicity of the catalyst materials and hence, higher activity is observed. Diglycerol monocarbonate has been observed as a reaction intermediate. The hydrotalcite materials can be easily recovered after reaction and re-used without any further activation treatment, whilst still displaying their high selectivity. A small drop in activity is observed during catalyst re-use, and this is more evident in the materials of lower basicity. Diglycerol dicarbonate has the potential to play an important role as a monomer for the production of non-isocyanate based polyurethanes, which makes it a highly desirable product, whilst also adding value to the waste stream of biodiesel production.

Acknowledgements

This work is part of the Biobased Performance Materials research programme, project no. BPM-013 “NOPANIC”, and financially supported by the Dutch Ministry of Economic Affairs. The authors would like to extend their gratitude to this consortium for funding. The authors would also like to thank Ing. L. Gootjes and Dr. D.S. van Es from Wageningen WUR–Food & Biobased Research for providing an authentic sample of DGDC.

References

- [1] C.H. Zhou, H. Zhao, D.S. Tong, L.M. Wu, W.H. Yu, *Catal. Rev. Sci. Eng.* 55 (2013) 369–453.
- [2] M. Pagliaro, M. Rossi, *Future of Glycerol*, The Royal society of Chemistry, 2008.
- [3] H.W. Tan, A.R. Abdul Aziz, M.K. Aroua, *Ren. Sust. Ener. Rev.* 27 (2013) 118–127.
- [4] A. Pilzecker, Brussels (2011). <http://www.ebb-eu.org/EBBpressreleases/Future%20of%20biofuels-Agricultural%20policy%20perspective.%20Pilzecker.pdf> - accessed 28.02.2014.
- [5] J.J. Bozell, G.R. Petersen, *Green Chem.* 12 (2010) 539–554.
- [6] R. Garcia, M. Besson, P. Gallezot, *Appl. Catal. A* 127 (1995) 165–176.
- [7] S. Carrettin, P. McMorn, P. Johnston, K. Griffin, G.J. Hutchings, *Chem. Commun.* (2002) 696–697.
- [8] F. Porta, L. Prati, *J. Catal.* 224 (2004) 397–403.
- [9] B. Katryniok, H. Kimura, E. Skrzynska, J.-S. Girardon, P. Fongarland, M. Capron, R. Ducoulombier, N. Mimura, S. Paul, F. Dumeignil, *Green Chem.* 13 (2011) 1960–1979.
- [10] M.A. Dasari, P.-P. Kiatsimkul, W.R. Sutterlin, G.J. Suppes, *Appl. Catal. A* 281 (2005) 225–231.
- [11] J. Chaminand, L. Djakovitch, P. Gallezot, P. Marion, C. Pinel, C. Rosier, *Green Chem.* 6 (2004) 359–361.
- [12] T. Miyazawa, Y. Kusunoki, K. Kunimori, K. Tomishige, *J. Catal.* 240 (2006) 213–221.
- [13] T. Kurosaka, H. Maruyama, I. Naribayashi, Y. Sasaki, *Catal. Commun.* 9 (2008) 1360–1363.
- [14] A.M. Ruppert, K. Weinberg, R. Palkovits, *Angew. Chem. Int. Ed.* 51 (2012) 2564–2601.
- [15] B. Katryniok, S. Paul, M. Capron, F. Dumeignil, *ChemSusChem* 2 (2009) 719–730.
- [16] L. Ott, M. Bicker, H. Vogel, *Green Chem.* 8 (2006) 214–220.
- [17] E. Tsukuda, S. Sato, R. Takahashi, T. Sodesawa, *Catal. Commun.* 8 (2007) 1349–1353.
- [18] S.-H. Chai, H.-P. Wang, Y. Liang, B.-Q. Xu, *Green Chem.* 9 (2007) 1130–1136.
- [19] B. Katryniok, S. Paul, V. Belliere-Baca, P. Rey, F. Dumeignil, *Green Chem.* 12 (2010) 2079–2098.
- [20] M.O. Sonnat, S. Amigoni, E.P. Taffin de Givenchy, T. Darmanin, O. Choulet, F. Guittard, *Green Chem.* 15 (2013) 283–306.
- [21] J.R. Ochoa-Gómez, O. Gómez-Jiménez-Aberasturi, C. Ramírez-López, M. Belsué, *Org. Process Res. Dev.* 16 (2012) 389–399.
- [22] A. Martin, M. Richter, *Eur. J. Lipid Sci. Technol.* 113 (2011) 100–117.
- [23] A.M. Ruppert, J.D. Meeldijk, B.W.M. Kuipers, B.H. Erné, B.M. Weckhuysen, *Chem. Eur. J.* 14 (2008) 2016–2024.
- [24] O. Kreye, H. Mutlu, M.A.R. Meier, *Green Chem.* 15 (2013) 1431–1455.
- [25] M.J. Climent, A. Corma, P. De Frutos, S. Iborra, M. Noy, A. Velty, P. Concepción, *J. Catal.* 269 (2010) 140–149.
- [26] A. Takagaki, K. Iwatani, S. Nishimura, K. Ebitani, *Green Chem.* 12 (2010) 578–581.
- [27] K. Lee, C.-H. Park, E. Lee, *Bioprocess Biosyst. Eng.* 33 (2010) 1059–1065.
- [28] J.J. McKetta, *Encyclopaedia of Chemical Processing and Design*, 1984, New York.
- [29] J. George, Y. Patel, S.M. Pillai, P. Munshi, *J. Mol. Catal. A* 304 (2009) 1–7.
- [30] J. Li, T. Wang, *J. Chem. Thermodyn.* 43 (2011) 731–736.
- [31] J.H. Teles, N. Rieber, W. Harder, in: U. Pat (Ed.), 1994. Patent number US 5359094 A.
- [32] J. Hu, J. Li, Y. Gu, Z. Guan, W. Mo, Y. Ni, T. Li, G. Li, *Appl. Catal. A* 386 (2010) 188–193.
- [33] H.-J. Cho, H.-M. Kwon, J. Tharun, D.-W. Park, *J. Ind. Eng. Chem.* 16 (2010) 679–683.
- [34] H. Corporation, *JEFFSOL® Alkylene Carbonates*, 2001.
- [35] E.-H. Lee, J.-Y. Ahn, M.M. Dharman, D.-W. Park, S.-W. Park, I. Kim, *Catal. Today* 131 (2008) 130–134.
- [36] C. Hammond, J.A. Lopez-Sanchez, M. Hasbi Ab Rahim, N. Dimitratos, R.L. Jenkins, A.F. Carley, Q. He, C.J. Kiely, D.W. Knight, G.J. Hutchings, *Dalton Trans.* 40 (2011) 3927–3930.
- [37] J.R. Ochoa-Gómez, O. Gómez-Jiménez-Aberasturi, B. Maestro-Madurga, A. Pesquera-Rodríguez, C. Ramírez-López, L. Lorenzo-Ibarreta, J. Torrecilla-Soria, M.C. Villarín-Velasco, *Appl. Catal. A* 366 (2009) 315–324.
- [38] M. Malyadri, K. Jagadeeswarai, P.S. Sai Prasad, N. Lingaiah, *Appl. Catal. A* 401 (2011) 153–157.
- [39] D.P. Debecker, E.M. Gaigneaux, G. Busca, *Chem. Eur. J.* 15 (2009) 3920–3930.
- [40] F. Cavani, F. Trifirò, A. Vaccari, *Catal. Today* 11 (1991) 173–301.
- [41] C.M. Janet, B. Viswanathan, R.P. Viswanath, T.K. Varadarajan, *J. Phys. Chem. C* 111 (2007) 10267–10272.
- [42] J.-M. Oh, S.-H. Hwang, J.-H. Choy, *Solid State Ionics* 151 (2002) 285–291.
- [43] W. Xie, H. Peng, L. Chen, *J. Mol. Catal. A* 246 (2006) 24–32.
- [44] F. Winter, X. Xia, B.P.C. Hereijgers, J.H. Bitter, A.J. van Dillen, M. Muhler, K.P. de Jong, *J. Phys. Chem. B* 110 (2006) 9211–9220.
- [45] S. Abello, F. Medina, D. Tichit, J. Perez-Ramirez, Y. Cesteros, P. Salagre, J.E. Sueiras, *Chem. Commun.* (2005) 1453–1455.
- [46] M.G. Alvarez, A.M. Segarra, S. Contreras, J.E. Sueiras, F. Medina, F. Figueras, *Chem. Eng. J.* 161 (2010) 340–345.
- [47] J.C.A.A. Roelofs, J.A. van Bokhoven, A.J. van Dillen, J.W. Geus, K.P. de Jong, *Chem. Eur. J.* 8 (2002) 5571–5580.